INFOGAIN PUBLICATION

International Journal of Advanced Engineering, Management and Science (IJAEMS)
Peer-Reviewed Journal
ISSN: 2454-1311 | Vol-7, Issue-10; Oct, 2021
Journal Home Page: https://ijaems.com/
Article DOI: https://dx.doi.org/10.22161/ijaems.710.1

Field Survey of Defects in RC Bridges

Hadeer M. El-Farargy[1], Al-Sayed E. El-kasaby[1] and Adel M. El-Kelesh[2]

[1]Department of Civil Engineering, Benha Faculty of Engineering, Benha University, Egypt
[2]Construction Engineering and Utilities Department, Faculty of Engineering and Geo-Construction Research and Development Center (GRDC-ZU), Zagazig University, Egypt

Received: 10 Sep 2021; Received in revised form: 08 Oct 2021; Accepted: 14 Oct 2021; Available online: 24 Oct 2021

Abstract— *Egypt has a large road network on which more than 3,000 bridges are in service. To provide for safe and functional bridges, periodic inspection and assessment of bridge condition is essential. This paper presents the results of a part of on-going research project in which seven RC bridges in Egypt were visually inspected in 2019 and 2020. The inspection results are used to survey the types and quantities of defects that are common in different elements of RC bridges. The defects that were surveyed in the current investigation include spalling of concrete with and without exposed rebar; wear and pothole in wearing surface; distortion and connection in metal railing; crack, delamination and spalling in median barrier; and wear, spalling and settlement in curbs and sidewalks. The inspection results are further used to determine the densities of these defects in the main elements of RC bridges. Discussion is also made on the evolution of defects with aging of bridges.*

Keywords— ***Bridge, Defects, Visual Inspection, Condition Rating.***

I. INTRODUCTION

According to GARBLT (2015b), Egypt has a road network of more than 64,000 km across the country, on which more than 3,000 bridges are in service. The reinforced concrete (RC) bridges represent approximately 90% of the bridges in Egypt (GARBLT 2015b). Moreover, the road networks and their bridges have increased largely during the last decade. These bridges differ in type, capacity, age and condition. Accidents occur because of deterioration or failure of roads or bridges. Since 1992 and for 20 years, the victims of roads and bridges in Egypt counted approximately 245000 people dead and 73000 injured. This represents 25 times the global rate (Al-Ahram 2015).

Over their lifetime, bridges deteriorate as a result of structural damage and/or material degradation and other causes. Therefore, timely action for maintenance, repair or rehabilitation is essential. This provides for safe and functional bridges. This necessitates a management tool to effectively inspect, manage and maintain bridges within imposed constrains (mainly budgetary constraints). A reliable bridge management system (BMS) for inspecting, managing and maintaining the bridge networks in Egypt has not yet been established. Inspections are usually made in response to warnings received from sources very often outside the bridge network system, or as a result of obvious inadequacy of a bridge to fulfill its expected function. Many bridges in Egypt suffer from major problems because of insufficient periodic inspection and maintenance (Elfahham 2016). This is mainly attributed to the shortage of skilled and well-trained human resources and equipment that are necessary for proper inspection and assessment of the conditions of bridges (GARBLT 2015b). The problem is exacerbated by the unavailability of clear strategy to conduct periodic inspection and maintenance in the right time.

Therefore, maintenance and management of the existing bridges has been a great concern for the Egyptian government and the public alike. In collaboration between the General Authority for Roads, Bridges and Land Transport (GARBLT) and Japan International Cooperation Agency (JICA), a number of bridges were inspected in the period 2013–2015 for the purpose of establishing inventory data of the bridges on regional roads of the country. This has been challenged by the scarcity of bridges' data and the large number of bridges in the network that needed much efforts and time to be surveyed

(Elfahham 2016). Since 2015 several bridges on the railway network have been inspected through collaborations between the National Authority for Egypt's Railways and Egyptian universities. This has been made for the purpose of evaluating the structural conditions of these bridges and proposing schemes for appropriate maintenance and repair works. The Board of Governors in 2015 established a working group to coordinate between the Ministry of Transportation and the Ministry of Higher Education for the development of a strategy and executive program for the evaluation and maintenance of the bridges in Egypt.

Research efforts have been made to establish systems for bridge management in Egypt (e.g., Abu-Hamd 2006; Abbas 2012; GARBLT 2015a; Elfahham 2016; Mansour et al. 2019). These efforts have contributed to the community of bridge engineering and management in Egypt. However, the developed systems have not accounted for important factors such as material vulnerability (Abbas 2012; GARBLT 2015a; Elfahham 2016), inspection quality (Abbas 2012; GARBLT 2015a; Elfahham 2016), environmental conditions (Abbas 2012, Final Seminar 2015), aging (Abbas 2012; Final Seminar 2015; Elfahham 2016), functional efficiency and client requirements (GARBLT 2015a). Moreover, the applicability of these systems has not been evaluated especially in terms of the inspection method and outputs, effect of environmental conditions on bridge deterioration, and bridge defects that are common in Egypt.

Inspection of bridges is an essential element of any BMS especially for aged and deteriorated bridges. Assessment and rating of bridges are based on the results of adopted inspection. The accuracy of bridge condition assessment relies heavily on the quality of inspection (Branco and de Brito 2004; Rashidi and Gibson 2011). Therefore, the heart of a BMS is the database derived from regular inspection and maintenance activities. The integrity of a BMS is directly related to the quality and accuracy of the bridge inventory and physical condition data obtained through field inspections (AASHTO 1994).

This paper presents the results of a part of on-going research project that aims at establishing a practical BMS for the RC bridges in Egypt. The main objectives of this project include the development of database of bridge deterioration data with time, determination of appropriate inspection methodology and period, determination of the factors that significantly affect the deterioration of bridges and evaluation of their effects, determination of the bridge defects that are common and critical, and evaluation of bridge deterioration with age. The current paper presents the results of visual inspections made in 2019 and 2020 on seven RC bridges in Egypt. These results are used to quantitatively evaluate the defects in the elements of the bridges. Discussions are made on the common types of defects, their causes and their evolution with time.

II. BACKGROUND

2.1 Condition Rating and Inspection

The condition of any component of a bridge may have an impact on the integrity or safety of the structure (e.g., Laman and Guyer 2010; Sutton et al. 2013). Therefore, the condition of a bridge and its elements must be inspected or monitored and evaluated regularly. This ensures the safety and functionality of bridges or determines the priorities for maintenance, repair or rehabilitation. Having sufficient inventory data such as traffic volume information, structural characteristics and bridge sketches as well as reliable data gathered through inspection, the condition of a bridge can be assessed (e.g., Suksuwan and Hadikusumo 2010; Adhikari et al. 2012).

Visual inspection (VI) is considered as the basic and prevalent technique of bridge inspection (e.g., Gattulli and Chiaramonte 2005; Liu et al. 2011). The funds, time and efforts involved in experimental investigations render VI more practical and appealing for bridge inspection. Currently available BMSs such as the earliest Pontis (Thompson et al. 1998) and BRIDGIT (Hawk and Small 1998; Small 2002) as well as the Finnish (Söderqvist and Veijola 1998), Danish (Lauridsen et al. 1998), German (Haardt 2002) and Japanese (Miyamoto et al. 2000) BMSs rely primarily on information obtained through visual inspection. The objective of VI is to evaluate the physical condition of a bridge. It is usually done on a routine basis by inspectors to detect and evaluate the deterioration and spot damages on the different structural elements of a bridge; most bridge defects (such as cracks, spalls and leaching) can be visually detected.

2.2 Common Bridge Defects

Bridges deteriorate because of many potential causes. Examples of such causes include chloride contamination, freeze-thaw, alkali-silica reaction, ettringite formation, collision damage, overload damage, carbonation, chemical attack, moisture absorption, differential foundation movement, design and construction deficiencies, temperature changes and fire damage (FHWA 2012). These causes result in defects in the elements of bridges. For the purpose of assessing the condition of a bridge, the defects need to be surveyed through inspection.

Several efforts have been made to survey and classify the common defects of RC bridges. Suksuwan and Hadikusumo (2010) used historical VI data of bridges in Thailand to survey and classify the types of defects that

potentially contribute to the deteriorations of different bridge elements. This was supported by suggestions and recommendations from interviews with experts. They reported that the common defects in columns include cracking of concrete because of shrinkage and temperature variation, scaling and wearing of concrete cover, porous material because of deteriorated and aged concrete, delamination of concrete cover, spalling and popouts of concrete cover. For deck slab, the defects include porous material because of deteriorated and aged concrete, spalling and popouts of concrete cover, potholes of the bridge deck, cracks and spalls around expansion joint of slabs, cracks and spalls at the end of deck over the cap beam, corrosion, and rusting of reinforcing steel. As for the wearing surface, the defects include friction loss because of polished aggregate, raveling because of loss of adhesion, corrugation of asphalt concrete surface and damaged patching of repaired area.

Rashidi and Gibson (2011) reported that the common defects of concrete bridges may be classified into discoloration, efflorescence, cracking and spalls, corrosion of non-prestressed reinforcement or deterioration of the prestress system and delamination. Moufti (2013) reported that the defects that are common in RC bridge elements include the following:

- Structural concrete elements: scaling, corrosion of reinforcement, pop-outs, cracking, delamination/ spalling, erosion and wet areas.
- Wearing surfaces: cracking, potholes, rutting, rippling and loss of bond.
- Drainage systems: pipe breakage, loosening/deterioration of components or connections or fasteners.
- Bearings: cracking, deformations, scouring/scratches, corrosion and bending/cracking of anchor bolts/welds.

Elfahham (2016) reported the following defects in concrete bridges: concrete cracking, concrete carbonation, concrete efflorescence, chloride contamination, alkali-Silica reaction (ASR), reinforcement steel corrosion, deteriorated joint seal, deteriorated expansion joint, defective drainage system, defective lighting unit, defective connections, defective prestressing cable anchors, misalignment, settlement, scour, leakage, dirt and debris, deck traffic impact (load capacity), deck deflection, deck delamination/spalling, substructure traffic impact, superstructure traffic impact.

However, little effort has been made to evaluate the densities of the defects that are common in the different elements of RC bridges. This is important in assessing the severity of the condition of a bridge element. Tuttle (2005) conducted visual inspections and survey of defects in sections of bridge decks. The defects were compiled with photographs. The types and locations of the defects were documented on defect survey worksheets. Measurements were taken on the top surfaces of the decks. The records included crack width and locations of delamination and potholes. These records were used to calculate the average crack density, crack severity and pothole density.

III. INSPECTION METHODOLOGY

In the current investigation, seven RC bridges (B1–B7) were visually inspected. The bridges are located on the ring road in the Greater Cairo as shown in Fig. 1. The ring road is a peripheral road connecting the governorates of the Greater Cairo. The seven bridges were selected for this investigation because of two main reasons: (1) many defects were clearly visible in the bridges at the time of inspection, and (2) they are located on the ring road which is a vital and important road in Cairo. The inventory data of the seven bridges are summarized in Table 1. They consist of general information, bridge characteristics and environmental conditions. The general information include the bridge number, bridge name, city, district, road name, year built, obstacle/crossing, previous owner, current owner, previous inspection and previous MR&R. The bridge characteristics include the structure type, material, construction method, length, width, vertical clearance, median width, sidewalk width, number of lanes, design load and general planning. According to Rashidi (2013), the environmental conditions include the environmental actions that cause chemical and physical deterioration of concrete. The degradation mechanism is usually related to the interaction between the environment and the material. The interaction with the environment is usually associated with climatic condition, air, aggressive soil cause, chemical reaction within concrete and human actions.

B2, B5 and B7 consist of two, six and single spans, respectively. All spans of the three bridges were inspected. B1 consists of three spans. A single span of B1 was inspected. B6 consists of sixteen spans. A single span of B6 was inspected. Both of B3 and B4 consist of five spans. The spans of B3 and B4 were inspected**.** Inspection included all the visible components which are the deck, superstructure and substructure. The foundations of the bridges could not be inspected. Inspection was made in two stages. The first was made from under the deck of a bridge. This consisted of visual inspection of the bottom of the deck, superstructure and substructure. For the superstructure, the beams/girders were inspected. However, the bearings were not clearly visible and

therefore could not be inspected. As for the substructure, the piers, bents, pier walls, pier caps and abutments were inspected. The foundations could not be inspected. In the second stage, inspection was made on the top surface of a bridge. This consisted of inspection of the wearing surface, railing, median barriers, curbs/sidewalks and expansion joints.

The seven bridges were inspected twice: in July 2019 and August 2020. The defects were surveyed for every inspected element. The characteristics of each defect were also recorded and described. The defects were then classified according to AASHTO (2011) and NJDOT (2015). A metric laser was used to measure the dimensions of a defect, such as the length and width as well as the depth if any. The severity of a defect was described on the basis of the guidelines of AASHTO (2011) and NJDOT (2015). It is worth mentioning that the inspection methodology and guidelines of AASHT (2011) and NJDOT (2015) are followed in most of the reported studies and inspections as they provide for reduced subjectivity and uncertainty.

IV. INSPECTION RESULTS

Examples of the defects surveyed in the inspections of the girders of B6 and deck slab of B7 in 2020 are shown in Figs. 2 and 3, respectively. The results of the visual inspection made in 2019, for example, are summarized in Tables 2 through 4. The total number of defects in each element of the seven bridges is shown in Table 2. Table 3 shows the types of defects in each element of the seven bridges. However, the number of each defect type is shown in Table 4 for every element of the seven bridges. In the remaining part of this section, the results of the inspections made in 2019 and 2020 are presented and described for each defect.

4.1 Spalling Density

The percentage of spalling density (SD) was calculated for the inspected decks, girders, piers, pier caps and abutments of the seven bridges (B1 through B7). It was calculated following the method of AASHTO (2011). For decks, it was calculated by dividing the quantity of spalling in square meters by the total area of deck. However, for girders it was calculated by dividing the quantity of spalling in meter by the total length of girders. For bents/piers it was calculated by dividing the quantity of spalling in square meters by the total area of bents/piers. For pier walls it was calculated by dividing the quantity of spalling in square meters by the total area of pier walls. For abutments it was calculated by dividing the quantity of spalling in meter by the total length of abutments.

The calculated SD is represented in Figs. 4 and 5 for the inspections of 2019 and 2020, respectively. No spalling was observed in the decks of B2, B5 and B6. For the decks of the other bridges, it is seen that SD ranges from 0.003 to 0.32%. Significant SD was observed in the girders of all bridges. It ranges from 2.67 to 76.30%. The greatest percentages were observed in the girders of B3 and B4. For the bents, piers and pier walls, the figures show no spalling for B1, B4 and B6. However, for the other bridges, the percentage ranges from 0.04 to 0.49%. No spalling was observed in the pier caps of all bridges. For the abutments, SD of approximately 6.25% was observed only in B5.

A comparison between the results in Figs. 4 and 5 shows useful observations on the effect of time (aging) on SD in RC bridges. For decks, very small increases of SD are observed. It increased from 0.0 to 0.09%, 0.0 to 0.05% and 0.32 to 0.40% in the decks of B2, B6 and B7, respectively. No increases were observed in the decks of the other bridges. However, for girders significant increases of SD were observed in most of the inspected bridges. SD of girders increased from 3.10 to 7.60%, 4.16 to 6.92%, 66.60 to 79.90%, 7.36 to 22.29% and 20.20 to 24.25% in B1, B2, B3, B6 and B7, respectively. No significant increases were observed in the girders of B4 and B5. For the bents, piers and pier walls very small increases of SD were observed because of time. SD increased from 0.29 to 0.58%, 0.0 to 0.15% and 0.0 to 0.03% for B3, B4 and B6, respectively. No increases were observed for the other bridges. Figures 4 and 5 show no appreciable increase of SD in the pier caps and abutments for all the inspected bridges.

4.2 Spalling Density without Exposed Rebar

The percentage of spalling density without exposed rebar (SDOER) was calculated for the inspected decks, girders, piers, pier caps and abutments. The calculation of SDOER was exactly the same way as that of SD; SDOER is only for the spalling without exposed rebar. The calculated SDOER is represented in Figs. 6 and 7 for the inspections of 2019 and 2020, respectively. For the decks, SDOER ranges from 0.003 to 0.25%. No SDOER was observed in the girder of B5. For the girders of the other bridges, SDOER ranges from 0.55 to 76.30%. For the bents, piers and pier walls, SDOER of approximately 0.04 and 0.49 was observed only in B2 and B5, respectively. No SDOER was observed in the abutments of all bridges.

A comparison between the results in Figs. 6 and 7 indicates the effect of time (aging) on SDOER. For decks, very small increases of SDOER because of time are observed. It increased from 0.0 to 0.009% and 0.006 to 0.042% in the decks of B6 and B7, respectively. No

significant increases are observed in decks of the other bridges. However, for girders, SDOER increased from 0.55 to 2.10% and 66.60 to 79.90% in B2 and B3, respectively. No significant increases are observed in the girders of the other bridges. Figures 6 and 7 show no appreciable increase of SDOER in the bents, piers and pier walls and abutments for all the inspected bridges.

4.3 Spalling Density with Exposed Rebar

The percentage of spalling density with exposed rebar (SDWER) was calculated for the inspected decks, girders, piers, pier caps and abutments. The calculation of SDWER was exactly the same way as that of SD; SDWER is only for the spalling with exposed rebar. The calculated SDWER is represented in Figs. 8 and 9 for the inspections of 2019 and 2020, respectively. No significant SDWER can be seen in the decks of B3 and B4. For the decks of the other bridges, SDWER of approximately 0.002 and 0.31% is observed in B1 and B7. No significant SDWER can be seen in the girders of B3, B4 and B7. For the girders of the other bridges, SDWER ranges from 2.00 to 5.76%. For the bents, piers and pier walls, SDWER of approximately 0.29% was observed only in B3. For the abutments, SDWER of approximately 6.25% was observed only in B5.

A comparison between the results in Figs. 8 and 9 reveals the effect of time (aging) on SDWER in RC bridges. For decks, very small increases of SDWER are observed. It increased from 0.0 to 0.09%, 0.0 to 0.04% and 0.31 to 0.36% in the decks of B2, B6 and B7, respectively. No increases are observed in the decks of the other bridges. However, for girders significant increases of SDWER are observed in most of the bridges. It increased from 2.00 to 6.94%, 3.61 to 4.82%, 5.67 to 22.08% and 0.0 to 5.00% for B1, B2, B6 and B7, respectively. For the bents, piers and pier walls very small increases of SDWER are observed because of time. It increased from 0.29 to 0.58%, 0.0 to 0.15% and 0.0 to 0.03% for B3, B4 and B6, respectively. No increases are observed for the other bridges. Also, no significant increase of SDWER can be seen in the abutments for all the inspected bridges.

4.4 Wear and Pothole Densities in Wearing Surface

The percentages of wear and pothole densities were calculated for the inspected wearing surfaces of B1 through B7. They were calculated following the method of AASHTO (2011). Wear density was calculated by dividing the quantity of wear in square meters by the total area of the wearing surface. Pothole density was calculated by dividing the quantity of pothole in square meters by the total area of the wearing surface. The calculated wear density is represented in Fig.10 for the inspections of 2019. It is seen that the wear density ranges from 50 to 100%. No significant pothole was observed in the wearing surfaces of all bridges in 2019. A comparison between the results of the inspections in 2019 and 2020 shows no appreciable increase of the wear density in the wearing surface for all the inspected bridges. However, a very small increase of the pothole density was observed because of time in the wearing surface of B2 only. It increased from 0.0 in 2019 to 0.03% in 2020.

4.5 Distortion and Connection Densities in Metal Railing

The percentages of distortion and connection densities were calculated for the inspected metal railings of the seven bridges. The distortion density was calculated by dividing the quantity of distortion in meter by the total length of metal railing. The connection density was calculated by dividing the quantity of connection in meter by the total length of metal railing. The calculated distortion and connection densities for the inspections of 2019 are represented in Figs. 11 and 12, respectively. It is seen that the distortion density ranges from 0.38 to 15.00%. No connection was observed in the metal railings of B2, B4 and B7. For the metal railings of the other bridges, the connection density ranges from 0.43 to 0.69% (see Fig. 12). A comparison between the results for the inspections of 2019 and 2020 shows no appreciable increase of distortion and connection densities in the metal railings for all the inspected bridges.

4.6 Cracks, Delamination and Spalling Densities in Median Barrier

The percentages of crack, delamination and spalling densities in median barrier were calculated for the seven bridges following the method of AASHTO (2011). The defect (crack, delamination or spalling) density was calculated by dividing the quantity of defect in meter by the total length of median barrier. As for the inspections of 2019, a crack density of approximately 1.89% was observed only in the median barrier of B1; there is no median barrier in B5. No delamination was observed in the median barriers of all bridges. No spalling was observed in the median barriers of B1, B3, B4 and B6. Spalling densities of approximately 5.00 and 6.82% were observed in the median barriers of B2 and B7, respectively. The inspections of 2020 indicated small increases of crack and delamination densities in the median barrier of B1. The crack density increased from 1.89 in 2019 to 5.03% in 2020. The delamination density increased from 0.0 in 2019 to 3.14% in 2020. No appreciable increase of spalling density was observed in 2020 in the median barriers of all bridges.

4.7 Wear, Spalling and Settlement Densities in RC Curbs and Sidewalks

The percentages of wear, spalling and settlement densities were calculated for the inspected RC curbs and sidewalks following the method of AASHTO (2011). The defect (wear, spalling or settlement) density was calculated by dividing the quantity of defect in meter by the total length of the RC curbs and sidewalks. The calculated wear and spalling densities of 2019 are represented in Figs. 13 and 14, respectively. It should be mentioned that the sidewalk of B1 was newly constructed at the time of inspection in 2019. Also, no defects were observed in the RC curbs and sidewalks of B6 in 2019. Figure 13 shows that the wear density ranges from 95.00 to 99.33%. Figure 14 also shows that the spalling density ranges from 0.67 to 5.00%. The inspections of 2020 revealed no appreciable increase in the wear, spalling or settlement in the RC curbs and sidewalks for all bridges. Also, because of planned expansion works no sidewalk was constructed in B7 in 2020.

V. ANALYSIS AND DISCUSSION

5.1 Spalling Density

On the basis of the results in Figs. 4 and 5, Table 5 summarizes the minimum, maximum and average values of SD for the inspected bridge elements. It is seen that SD in decks ranges from 0.0 to 0.32% with an average of 0.08% in 2019. However, it ranges from 0.0 to 0.40% with an average of 0.11% in 2020. It is worth mentioning that Tuttle (2005) reported SD of 0.42% for deck slabs. This is highly consistent with the above results. For girders, SD ranges from 2.67 to 76.30% with an average of 25.77% in 2019. It ranges from 2.67 to 79.90% with an average of 31.42% in 2020. As for the bents, piers and pier walls SD ranges from 0.0 to 0.49% with an average of 0.14% in 2019. In 2020, it ranges from 0.0 to 0.58% with an average of 0.21%. For abutments, SD ranges from 0.0 to 6.25% with an average of 1.56% in 2019 with no change in 2020.

The results in Figs. 4 and 5 reveal the following:

- For the deck slabs, the results of 2019 show that SD is the greatest for B7 (0.32%). Then, it decreases in order for B1 (0.25%), B3 (0.003%), B4 (0.003%), B2 (0.00), B5 (0.00) and B6 (0.00). The results of 2020 show that SD is the greatest for B7 (0.40%). Then, it decreases in order for B1 (0.25%), B2 (0.09%), B6 (0.05%), B3 (0.003%), B4 (0.003%) and B5 (0.00).
- For the girders, the results of 2019 indicate that SD in 2019 is the greatest for B4 (76.30%). Then it decreases in order for B3 (66.60%), B7 (20.20%), B6 (7.36%), B2 (4.16%), B1 (3.10%) and B5 (2.67%). However, the results of 2020 indicate that SD is the greatest for B3 (79.90%). Then, it decreases in order for B4 (76.30%), B7 (24.25%), B6 (22.29%), B1 (7.60%), B2 (6.92%) and B5 (2.67%).
- As for the bents, piers and pier walls, the results of 2019 show that SD is the greatest for B5 (0.49%). Then, it decreases in order for B3 (0.29%), B2 (0.04%), B1 (0.00), B4 (0.00) and B6 (0.00). The results of 2020 show that SD is the greatest for B3 (0.58%). Then, it decreases in order for B5 (0.49%), B4 (0.15%), B2 (0.04%), B6 (0.03%) and B1 (0.00).
- For the abutments, SD was observed only in B5 (6.25%) in 2019. No change was experienced in 2020.

A careful investigation and monitoring of the inspection sites indicated that spalling of concrete in the inspected bridges is attributed to several causes as follows:

- For the decks, spalling was attributed to rusting reinforcement as well as previous repair and development works.
- For the girders, spalling was attributed to several causes that include: age of bridge, impact by trucks, fire, environmental conditions and geometrical characteristics of bridge such as superelevation in bridge alignment. A truck impacts the bottom of a girder if the truck height exceeds the clear height of a bridge. The investigation and inspection revealed clear symptoms of impact at the bottom of the girders of B1, B2, B6 and B7. The spalling of concrete at the girders of B6 and B7 was significantly greater than that of B1 and B2. Impact may happen also in case of existence of asphalt overlay on the road below a bridge
- For the bents, piers and pier walls of B2, spalling was attributed to the cleaning works and equipment that were routinely done around the bridge. For B3 and B4, environmental factors and uncontrolled garbage were the main causes. For B5, spalling was caused by fire at the location of the bridge.

5.2 Spalling Density without Exposed Rebar

Table 6 shows that SDOER in the deck slabs ranges from 0.0 to 0.25% with an average of 0.04% in 2019 with no significant change in 2020. For girders, SDOER ranges from 0.00 to 76.30% with an average of 23.76% in 2019.

However, it ranges from 0.00 to 79.90% with an average of 25.49% in 2020. As for the bents, piers and pier walls SDOER ranges from 0.00 to 0.49% with an average of 0.09% in 2019 with no change in 2020. This indicates that SDOER in girders is largely greater than that in deck slabs.

For deck slabs, Fig. 6 shows for the inspections of 2019 that SDOER is the greatest for B1 (0.25%). Then, it decreases in order for B7 (0.01), B3 (0.003%), B4 (0.003%), B2 (0.00), B5 (0.00) and B6 (0.00). However, Fig. 7 shows for the inspections of 2020 that SDOER is the greatest for B1 (0.25%). Then, it decreases in order for B7 (0.04%), B6 (0.009%), B4 (0.003%), B3 (0.003%), B2 (0.00) and B5 (0.00). As for the girders, SDOER for the inspections of 2019 is the greatest for B4 (76.30%). Then, it decreases in order for B3 (66.60%), B7 (20.20%), B6 (1.60%), B1 (1.06%), B2 (0.55%) and B5 (0.00). However, SDOER for the inspections of 2020 is the greatest for B3 (79.90%). Then it decreases in order for B4 (76.30), B7 (19.25%), B2 (2.10%), B1 (0.66%), B6 (0.21%) and B5 (0.0). For the bents, piers and pier walls, it is seen for the inspections of 2019 that SDOER is the greatest for B5 (0.49). Then, it decreases to 0.04% for B2 and 0.00 for B1, B3, B4 and B6. SDOER did not experience significant changes in the period from July 2019 to August 2020.

5.3 Spalling Density with Exposed Rebar

Table 7 summarizes SDWER the inspected elements of the seven bridges. It shows for the inspections of 2019 that SDWER in deck slabs ranges from 0.0 to 0.31% with an average of 0.06%. However, for the inspections of 2020, it ranges from 0.0 to 0.36% with an average of 0.07%. For girders, SDWER ranges from 0.0 to 5.76% with an average of 2.01% in 2019. However, it ranges from 0.0 to 22.08% with an average of 5.93% in 2020. As for the bents, piers and pier walls, SDWER ranges from 0.0 to 0.29% with an average of 0.05% in 2019. It ranges from 0.0 to 0.58% with an average of 0.13% in 2020. For abutments, SDWER ranges from 0.0 to 6.25% with an average of 1.56% in 2019 with no significant change in 2020.

For deck slabs, Fig. 8 shows for the inspections of 2019 that SDWER is the greatest for B7 (0.31%). Then, it decreases to 0.002% for B1 and 0.00 for B2, B3, B4, B5 and B6. For the inspections of 2020, Fig. 9 shows that SDWER is the greatest for B7 (0.36%). Then, it decreases in order for B2 (0.09%), B6 (0.04%), B1 (0.002%), B3 (0.00), B4 (0.00) and B5 (0.00). As for girders, SDWER for the inspections of 2019 is the greatest for B6 (5.67%). Then, it decreases in order for B2 (3.61%), B5 (2.67%), B1 (2.00%), B3 (0.00), B4 (0.00) and B7 (0.00). For the inspections of 2020, SDWER is the greatest for B6 (22.08%). Then, it decreases in order for B1 (6.94%), B7 (5.00%), B2 (4.82), B5 (2.67%), B3 (0.00) and B4 (0.00). For bents, piers and pier walls, SDWER of 0.29% was observed only in B3 in 2019. However, for the inspections of 2020, SDWER is the greatest in B3 (0.58%). Then, it decreased in order for B4 (0.15%), B6 (0.03%), B2 (0.00) and B5 (0.00). For abutments, SDWER of 6.25% was observed only in B5 in 2019. It did not experience significant change in the period from July 2019 to August 2020.

5.4 Wear and Pothole Density in Wearing Surface

Table 8 indicates that the wear density in wearing surface ranges from 50 to 100% with an average of 71.43% for both inspections of 2019 and 2020. Figure 10 shows that the wear density in 2019 was approximately 100% for B3, B4 and B5, while it was approximately 50% for B1, B2, B6 and B7. The wear density did not experience significant change in the period from July 2019 to August 2020. Table 8 also shows that no pothole in the wearing surface was experienced in 2019. However, in 2020 it ranges from 0.0 to 0.03% with an average of 0.01%. This indicates that the density of wear is greater than that of pothole in wearing surfaces

5.5 Distortion and Connection Density in Metal Railing

Table 9 shows that the distortion density in metal railing ranges from 0.38 to 15.00% with an average of 5.00% in both of 2019 and 2020. However, the connection density ranges from 0.0 to 0.69% with an average of 0.34% in both of 2019 and 2020. This implies that the distortion density is greater than the connection density in metal railing. Figure 11 shows for the inspections of 2019 that the distortion density is the greatest for B2 (15%). Then, it decreases in order for B6 (7.78%), B1 (5.82%), B7 (4.55%), B5 (1.10%), B4 (0.39%) and B3 (0.38%) in both of 2019 and 2020. Figure 12 shows for the inspections of 2019 that the connection density is the greatest for B6 (0.69%). Then, it decreases in order for B1 (0.63%), B3 (0.63%), B5 (0.43%), B2 (0.00), B4 (0.00) and B7 (0.00). No significant changes in distortion or connection were experienced in the period from July 2019 to August 2020. Accident damage was the main cause for the defects in metal railing.

5.6 Crack, Delamination and Spalling Density in Median Barrier

Table 10 shows that the crack density in the median bridge barrier ranges from 0.0 to 1.89% with an average of 0.32% in 2019; cracks were observed only in B1. However, it ranges from 0.0 to 5.03% with an average of 0.84% in 2020. It is also seen in Table 10 that no delamination was experienced in the median barrier in 2019. However, the

delamination density ranges from 0.0 to 3.14% with an average of 0.52% in 2020. The inspection results of 2019 show that the spalling density in the median barrier ranges from 0.0 to 6.82% with an average of 1.97% in both of 2019 and 2020. The spalling density was the greatest for B7 (6.82%). Then, it decreased to 5.00% for B2 and 0.00 for B1, B3, B4 and B6. It is seen that density of spalling is greater than that of cracks. In addition, the density of cracks is greater than that of delamination. The cause for these defects in the median barrier was most likely impact of vehicles.

5.7 Wearing, Spalling and Settlement Density in Curbs and Sidewalks

The survey results of the defects in the curbs and sidewalks are summarized in Table 11.

The wear density ranges from 0.0 to 99.33% with an average of 69.83% in 2019. However, it ranges from 0.0 to 99.33% with an average of 65.19% in 2020. The spalling density ranges from 0.0 to 5.00% with an average of 1.60% in 2019. In 2020 it ranges from 0.0 to 5.00% with an average of 1.48%. It is seen that settlement density ranges from 0.0 to 99.33% with an average of 28.15% in 2019. However, it ranges from 0.0 to 99.33% with an average of 16.56% in 2020.

Figure 13 shows for the inspections of 2019 and 2020 that the wear density in the curbs and sidewalks is the greatest for B5 (99.33%). Then, it decreases in order for B4 (98.68%), B3 (98.13%), B7 (97.70%), B2 (95.00%), B1 (0.00) and B6 (0.00). As shown in Figure 14, the spalling density is the greatest for B2 (5.00%). Then, it decreases in order for B7 (2.30%), B3 (1.88%), B4 (1.32%), B5 (0.67%), B1 (0.00) and B6 (0.00) in 2019 and 2020. Table 11 indicates that among the defects of the sidewalk, the wear density is the greatest, the spalling density is the lowest, and the settlement density is intermediate. The main cause for the defects in the median barrier was most likely the traffic and impact of vehicles.

VI. CONCLUSIONS

The results of visual inspections made in 2019 and 2020 on seven RC bridges in Egypt are presented and discussed in this paper. The age of the inspected bridges is approximately 35 years. The inspection results were used to quantitatively survey the types and quantities of defects in the different elements of RC bridges. On the basis of the presented results and discussions, the main conclusions that can be drawn include the following:

- The common defects that were surveyed in the 35 year bridges are spalling of concrete with and without exposed rebar; wear and pothole in wearing surface; distortion and connection in metal railing; crack, delamination and spalling in median barrier; and wear, spalling and settlement in curbs and sidewalks.
- The density of concrete spalling in deck slabs and girders ranges from 0.00 to 0.40% and 2.67 to 79.90%, respectively. In bents, piers and pier walls it ranges from 0.0 to 0.58%. In abutments it ranges from 0.0 to 6.25%. The spalling of concrete in deck slabs is attributed to rusting reinforcement and previous repair and development works, while that in girders is attributed to age of bridge, impact by trucks, fire, environmental conditions and geometrical characteristics of bridge. For bents, piers and pier walls, spalling is attributed to cleaning works and equipment, environmental factors and fire.
- The density of wear and pothole in wearing surface ranges from 50.00 to 10.00% and 0.00 to 0.03%, respectively.
- The density of distortion and connection in metal railing range from 0.38 to 15.00% and 0.0 to 0.69%, respectively. Distortion and connection in metal railing are most likely attributed to damage by accidents.
- The density of crack, delamination and spalling in median barrier ranges from 0.0 to 5.03%, 0.0 to 3.14% and 0.0 to 6.82%, respectively. These are likely attributed to the impact of vehicles.
- The density of wear, spalling and settlement in curbs and sidewalks ranges from 0.0 to 99.33%, 0.0 to 5.00% and 0.0 to 99.33%, respectively. These defects are most likely attributed to the traffic and impact of vehicles.

REFERENCES

[1] AASHTO (1994). "Manual for Condition Evaluation of Bridges," Washington D.C: American Association of State Highway and Transportation Officials.

[2] AASHTO. (2011). "Manual for bridge evaluation," Washington, D.C: American Association of State Highway and Transportation Officials Subcommittee on, Bridges Structures.

[3] Abbas, O.S.M. (2012). "Towards an Egyptian bridge management system," M.Sc. Thesis, Cairo University.

[4] Abu-Hamd, I., Georgy, M., Amer, A., and Fadel, A. (2006). "A proposed bridge management system for Egypt," Proceedings of the International Conference on Bridge Management Systems, Monitoring, Assessment and Rehabilitation, RMIT University.

[5] Adhikari, R.S., Moselhi, O. and Bagchi, A. (2012). "Automated prediction of condition state rating in bridge inspection," Gerontechnology, 11(2), 81.
[6] Al-Ahram (2015). "Egypt is the first of the world in road and bridges accidents," Issue 8, May 2015, http://www.ahram.org.eg/NewsQ/386201.
[7] Branco, F.A., and Brito, J.D. (2004). "Handbook of concrete bridge management," American Society of Civil Engineers.
[8] ElFahham, Y.M.H. (2016). "Adaptive optimization of bridges maintenance under budget constraints in Egypt," Ph.D. Thesis, Alexandria University, Egypt.
[9] Federal Highway Administration (FHWA) (2012). "Bridge Inspector's Reference Manual," U.S. Department of Transportation, FHWA NHI 12–49.
[10] Gattulli, V. and Chiaramonte, L. (2005). "Condition assessment by visual inspection for a bridge management system," Computer-Aided Civil and Infrastructure Engineering, 20(2), 95–107.
[11] General Authority for Roads, Bridges and Land Transport (GARBLT) (2015a). "Final Seminar," The project for improvement of the bridge management capacity.
[12] General Authority for Roads, Bridges and Land Transport (GARBLT) (2015b). "The project for improvement of the bridge management capacity," Project Completion report, Arab Republic of Egypt.
[13] Haardt, P. (2002). "Development of a bridge management system for the German highway network," Proceedings of the First International Conference on Bridge Maintenance, Safety and Management.
[14] Hawk, H. and Small, E.P. (1998). "The BRIDGIT bridge management system," Structural Engineering International, 8(4), 309–314
[15] Laman, J.A. and Guyer, R.C. (2010). "Condition assessment of short-line railroad bridges in Pennsylvania," Pennsylvania: The Thomas D. Larson Pennsylvania Transportation Institute, The Pennsylvania State University.
[16] Lauridsen, J., Bjerrum, J. andersen, N.H. and Lassen, B. (1998). "Creating a bridge management system," Structural Engineering International, 8(3), 216–220.
[17] Liu, T.Y., Chiang, W.L., Chen, C.W., Hsu, W.K., Lu, L.C. and Chu, T.J. (2011). "RETRACTED: Identification and monitoring of bridge health from ambient vibration data," Journal of Vibration and Control, 17(4), 589–603.
[18] Mansour, D.M.M., Moustafa, I.M., Khalil, A.H., and Mahdi, H.A. (2019). "An assessment model for identifying maintenance priorities strategy for bridges," Ain Shams Engineering Journal, 10(4), 695–704.
[19] Miyamoto, A., Kawamura, K., and Nakamura, H. (2000). "Bridge management system and maintenance optimization for existing bridges," Computer-Aided Civil and Infrastructure Engineering, 15(1), 45–55.
[20] Moufti, S. (2013). "A defect-based approach for detailed condition assessment of concrete bridges," Ph.D. Thesis, Concordia University.
[21] NJDOT (2015)."Bridge element inspection manual," New Jersey Department of Transportation.
[22] Rashidi, M. (2013). "Decision support system for remediation of concrete bridges," Ph.D. Thesis, University of Wollongong, Australia.
[23] Rashidi, M. and Gibson P. (2011). "Proposal of a methodology for bridge condition assessment," Australasian Transport Research Forum (ATRF), Adelaide, Australia.
[24] Small, E. (2002). "Bridge management systems," Personal Communication.
[25] Söderqvist, M.K. and Veijola, M. (1998). "The Finnish bridge management system," Structural Engineering International, 8(4), 315–319.
[26] Suksuwan, N. and Hadikusumo, B.H. (2010). "Condition rating system for Thailand's concrete bridges," Journal of Construction in Developing Countries, 15(1), 1–27.
[27] Sutton, J.P., Mouras, J.M., Samaras, V.A., Williamson, E.B. and Frank, K.H. (2013). "Strength and Ductility of Shear Studs under Tensile Loading," Journal of Bridge Engineering, 19(2), 245–253.
[28] Thompson, P.D., Small, E.P., Johnson, M. and Marshall, A.R. (1998). "The Pontis bridge management system," Structural Engineering International, 8(4), 303–308.
[29] Tuttle, R.S. (2005)." Condition analysis of concrete bridge decks in Utah," M.Sc. Thesis, Brigham Young University.

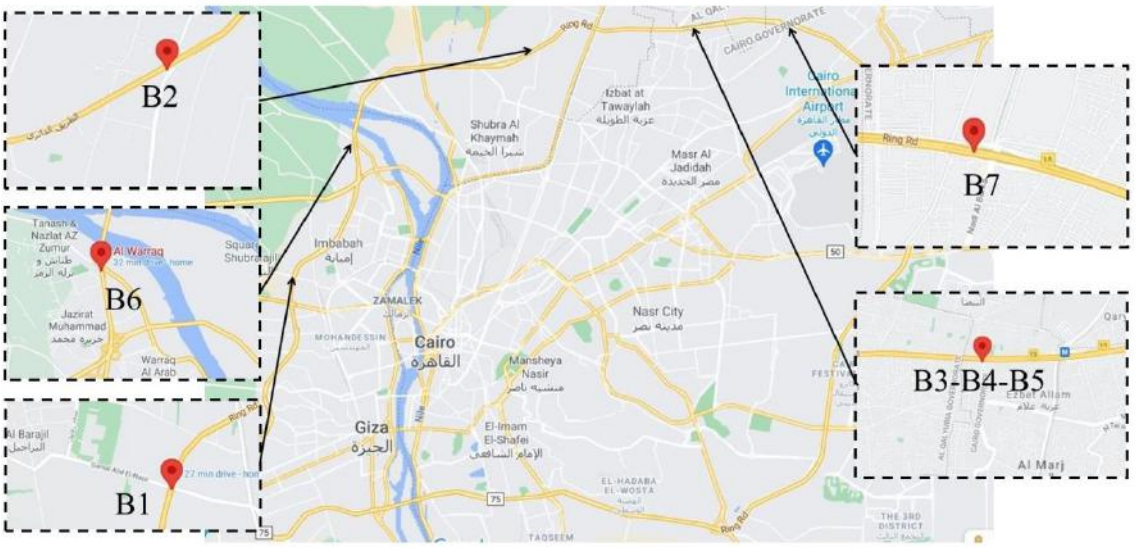

Fig.1: Map locations of seven inspected bridges on the ring road of the Greater Cairo

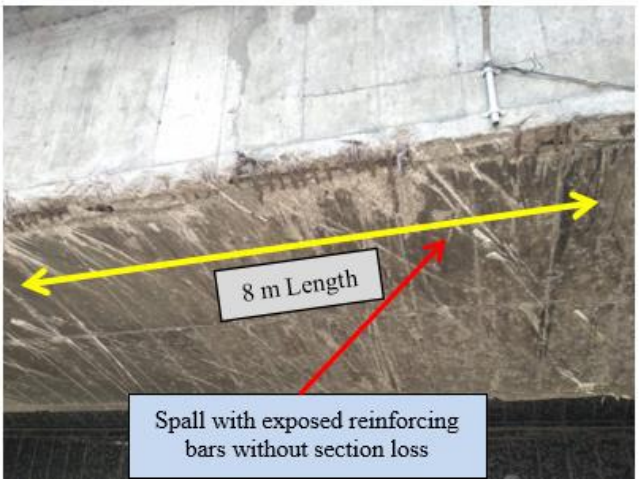

Fig.2: Example defects in girder of B6

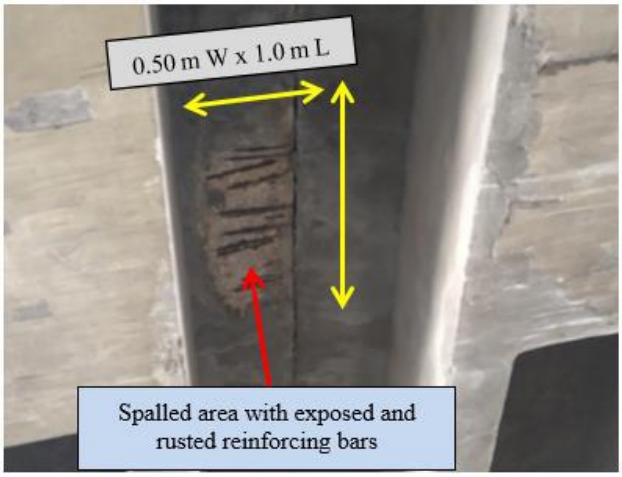

Fig.3: Example defects in deck slab of B7

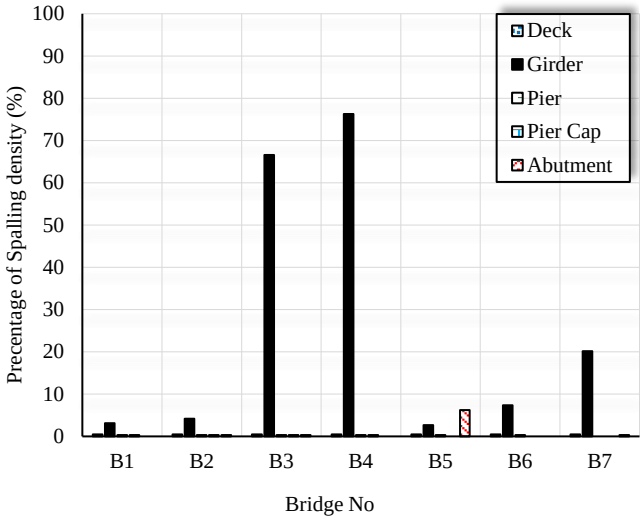

Fig.4: SD for elements of seven bridges inspected in July 2019

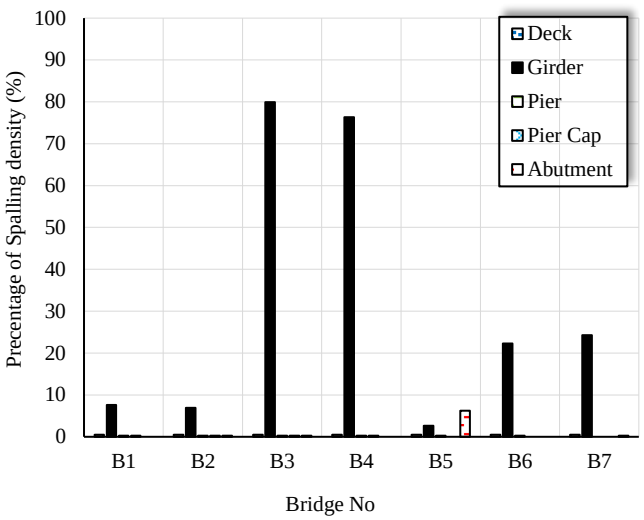

Fig.5: SD for elements of seven bridges inspected in August 2020

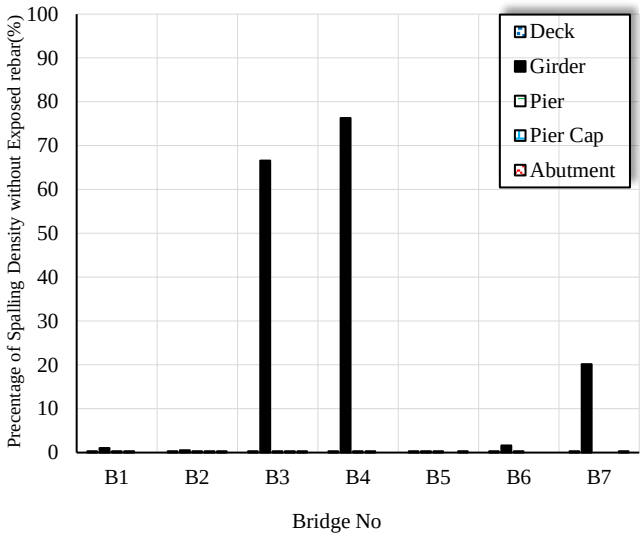

Fig.6: SDOER for elements of seven bridges inspected in July 2019

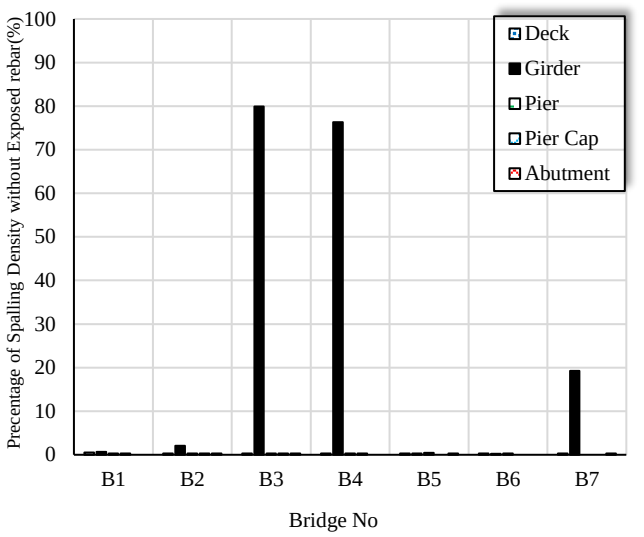

Fig.7: SDOER for elements of seven bridges inspected in August 2020

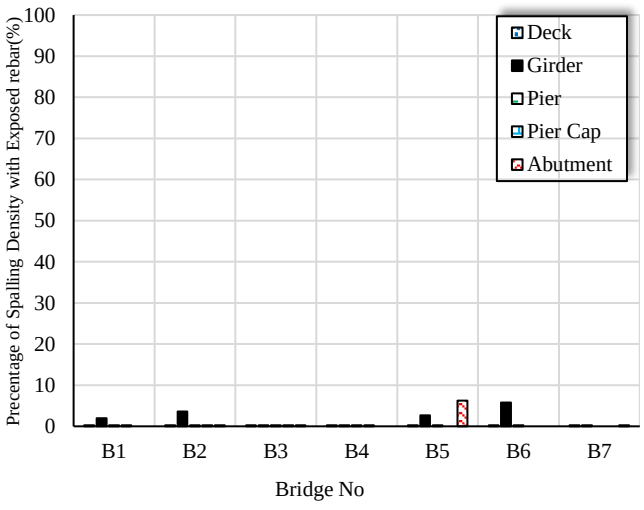

Fig.8: SDWER for elements of seven bridges inspected in July 2019

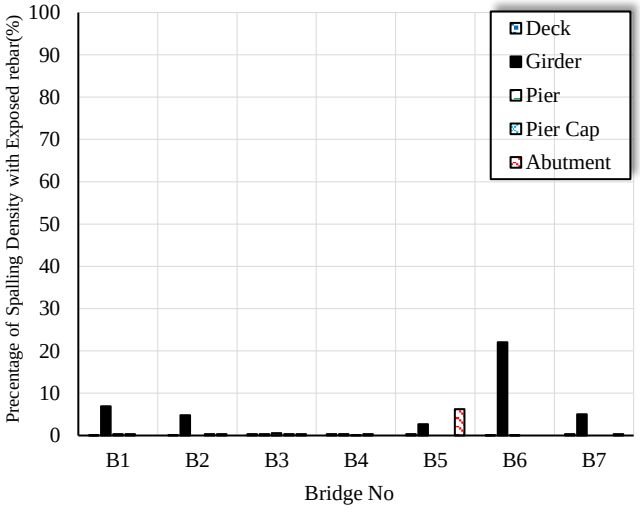

Fig.9: SDWER for elements of seven bridges inspected in August 2020

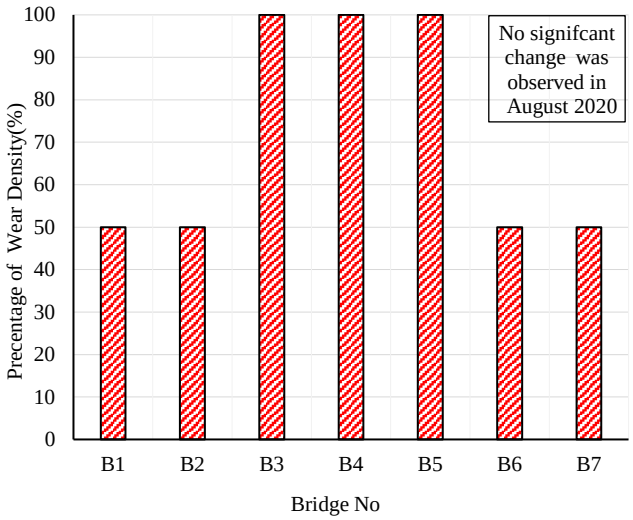

Fig.10: Wear density in wearing surfaces of seven bridges inspected in July 2019

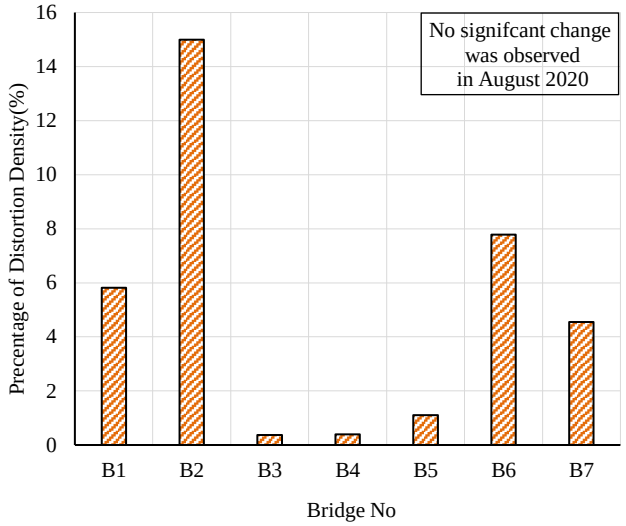

Fig.11: Distortion density in metal railing of seven bridges inspected in July 2019

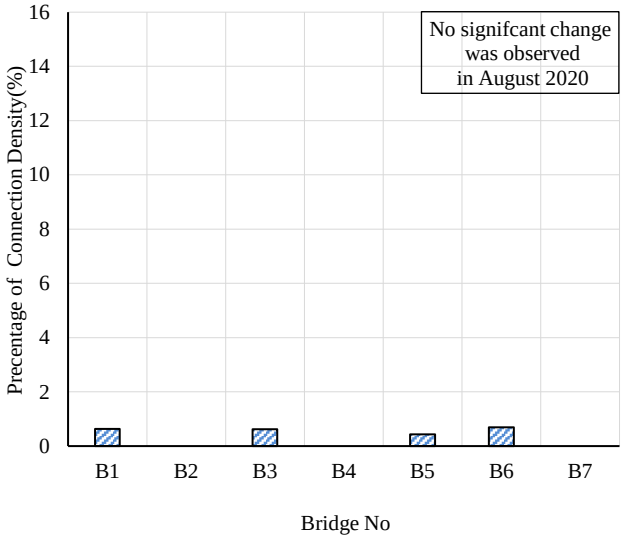

Fig.12: Connection density in metal railing of seven bridges inspected in July 2019

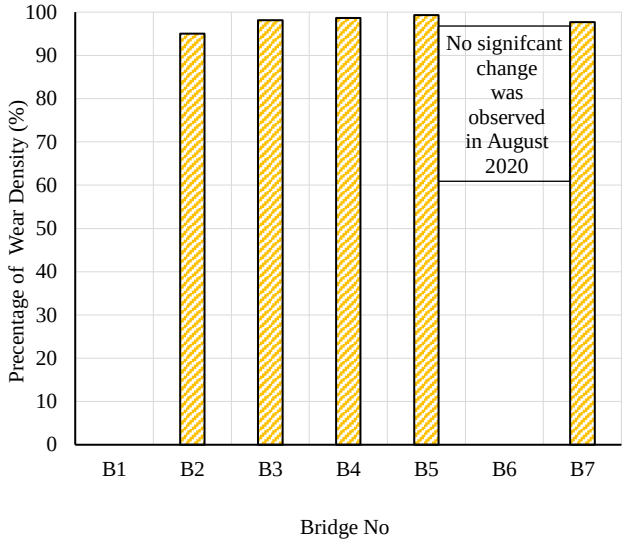

Fig.13: Wear in RC curbs and sidewalks of seven bridges inspected July 2019

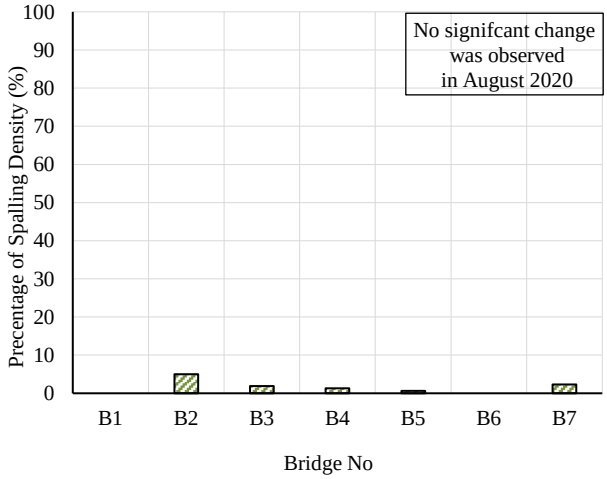

Fig.14: Spalling density in RC curbs and sidewalks of seven bridges inspected in July 2019

Table 1. Inventory data of seven inspected bridges on the ring road of the Greater Cairo

Bridge No	B1	B2	B3	B4	B5	B6	B7
Bridge Name	El Barajil	Bahteem	El Marg "part1"	El Marg "part 2"	El Marg "one way"	El Warraq	El Zakah
Location	El Barajil	Bahteem	El Marg	El Marg	El Marg	El Warraq	El Zakah
City	Giza	Qalyubia	Cairo	Cairo	Cairo	Qalyubia	Cairo
District	Embaba	East Shubra Al-Khaimah	El Marg	El Marg	El Marg	El Warraq	Al Salam
Road Name	Ring road	Ring road	Ring road	Ring road	Ring road	Ring road	Ring road
Year Built	1986	1986	1986	1986	1986	1986	1986
Obstacle/Crossing	Road way	Road way	Road way	Road way	Road way	water way	Road way
Previous Owner	Ministry of Housing	Ministry of Housing	Ministry of Housing	Ministry of Housing	Ministry of Housing	Ministry of Housing	Ministry of Housing
Current Owner	GARBLT	GARBLT	GARBLT	GARBLT	GARBLT	GARBLT	GARBLT
Previous Inspection	Yes	yes	Yes	yes	unknown	yes	yes
Previous MR&R	Yes	yes	Yes	no	unknown	yes	yes
Structure Type	Tee-beam type	Tee-beam type	Bulb –tee beam type	Bulb –tee beam type	Box- girder type	Box- girder type	Tee-beam type
Material	RC	RC	Prestressed	Prestressed	RC	Prestressed	RC
Construction Method	Conventional	conventional	conventional	conventional	conventional	conventional	conventional
Length (m)	17.5	19.0	40.0	38.0	150.0	36.0	22.0
Width (m)	39.3	61.0	50.0	50.0	9.0	50.0	44.0
Clearance (m)	5.0	5.1	5.3	5.3	-	5.6	5.3
Median Width (m)	0.5	0.5	0.5	0.5	N0	0.5	0.5
Sidewalk Width (m)	1.5	1.5	1.5	1.5	1.2 , 0.8	1.5	1.5
No. of Lanes	8	8	8	8	2	8	8
No. of Spans	3	2	5	5	6	16	1
Design Load (t)	70	70	70	70	70	70	70
General Planning	Horizontal	Horizontal	Vertical	Vertical	Horizontal	Vertical	Horizontal
Environment	High	High	Medium	Medium	High	High	High

Table 2. Number of defects in elements of seven bridges inspected in 2019

BRIDGE ELEMENT	B1	B2	B3	B4	B5	B6	B7
Deck	8	0	4	1	0	0	5
Girder	12	19	15	20	6	17	36
Pier, Bent or Pier Wall	0	3	2	2	2	0	-
Pier Cap	0	0	0	0	-	-	-
Abutment	-	0	0	-	2	-	0
Bearing	20	30	20	20	14	16	-
Wearing Surface	1	1	2	2	1	1	1
Bridge Railing	2	2	2	1	4	3	1
Median Barrier	1	2	0	0	-	0	2
Curbs/Sidewalk	0	2	2	2	3	0	3
Expansion Joint	0	0	-	-	2	-	0
Drainage							

Table 3. Type of defects in elements of seven bridges inspected in 2019

Bridge Element	B1	B2	B3	B4	B5	B6	B7
Deck	Spalling, Exposed Rebar	-	Spalling, Exposed Rebar	Spalling	-	-	Spalling, Exposed Rebar
Girder	Spalling, Exposed Rebar	Spalling, Exposed Rebar, Patched Area	Spalling,	Spalling	Spalling, Exposed Rebar	Spalling, Exposed Rebar, Patched Area	Spalling, Exposed Rebar, Patched Area
Pier or Bent or Pier Wall	-	Spalling	Spalling, Exposed Rebar	Spalling, Exposed Rebar	Spalling	-	-
Pier Cap	-	-	-	-	-	-	-
Abutment	-	-	-	-	Spalling, Exposed Rebar	-	-
Bearing	Movement "Minor Restriction"	Movement "Minor Restriction"	Movement "Minor Restriction"	Movement "Minor Restriction"	Movement "Minor Restriction"	Movement "Minor Restriction"	-
Wearing Surface	Wear "Minor Roughness"	Wear "Minor Roughness"	Wear "Minor Roughness", Rutting	Wear "Minor Roughness", Rutting	Wear "Minor Roughness"	Wear "Minor Roughness"	Wear "Minor Roughness"
Bridge Railing	Connection, Distortion	Distortion	Connection, Distortion	Distortion	Connection, Distortion	Connection, Distortion	Distortion
Median barrier	Cracks	Spalling, Exposed Rebar	-	-	-	-	Spalling, Exposed Rebar
Curbs/Sidewalk	-	Spalling, Wear	Spalling, Wear	Spalling, Wear	Spalling, Settlement, Wear	-	-

Expansion Joint	-	-	-	-	Debris Impaction	-	-
Drainage							

Table 4. Numbers of defect types in elements of seven bridges inspected in 2019

Element Description	Spalling	Exposed rebar	Patched Area	Movement	Wear	Pothole	Distortion	Connection	Settlement	Cracks	Debris impact
Deck "R.C Top-Flange"	12	6	0								
R.C Closed Web/Box Girder	98	19	9								
RC Pier Wall	7	2	0								
RC Open Abutment	1	1	0								
Disk Bearing				120							
Wearing Surface					9	0					
Metal Bridge Railing							10	5			
Median barrier	2	2							1		
RC Curbs &Sidewalks	4				4					1	
Assembly Joint without Seal											1
Compression Joint Seal											1

Table 5. Statistical values of SD in RC bridges inspected in 2019 and 2020

Date	Value	Deck	Girder	Bent/Pier/ Pier wall	Pier Cap	Abutment
July 2019	Minimum	0.0	2.67%	0.0	0.0	0.0
	Maximum	0.32%	76.30%	0.49	0.0	6.25%
	Average	0.08%	25.77%	0.14%	0.0	1.56%
	Standard Deviation	0.14	31.90	0.21	0.0	3.13

August 2020	Minimum	0.0	2.67%	0.0	0.0	0.0
	Maximum	0.40%	79.90%	0.58%	0.0	6.25%
	Average	0.11%	31.42%	0.21%	0.0	1.56%
	Standard Deviation	0.16	32.90	0.25	0.0	3.13

Table 6. Statistical values of SDOER in RC bridges inspected in 2019 and 2020

Date	Value	Deck	Girder	Bent/Pier/ Pier wall	Pier Cap	Abutment
July 2019	Minimum	0.0	0.0	0.0	0.0	0.0
	Maximum	0.25%	76.30%	0.49%	0.0	0.0
	Average	0.04%	23.76%	0.09%	0.0	0.0
	Standard Deviation	0.09	33.46	0.20	0.0	0.0
August 2020	Minimum	0.0	0.0	0.0	0.0	0.0
	Maximum	0.25%	79.90%	0.49%	0.0	0.0
	Average	0.04%	25.49%	0.09%	0.0	0.0
	Standard Deviation	0.09	36.59	0.20	0.0	0.0

Table 7. Statistical values of SDWER in RC bridges inspected in 2019 and 2020

Date	Value	Deck	Girder	Bent/Pier/ Pier wall	Pier Cap	Abutment
July 2019	Minimum	0.0	0.0	0.0	0.0	0.0
	Maximum	0.31%	5.76%	0.29%	0.0	6.25%
	Average	0.06%	2.01%	0.05%	0.0	1.56%
	Standard Deviation	0.12	2.21	0.12	0.0	3.13
August 2020	Minimum	0.0	0.0	0.0	0.0	0.0
	Maximum	0.36%	22.08%	0.58%	0.0	6.25%
	Average	0.07%	5.93%	0.13%	0.0	1.56%
	Standard Deviation	0.13	7.58	0.23	0.0	3.13

Table 8. Statistical values of wear and pothole density in wearing surface of RC bridges inspected in 2019 and 2020

Date	Value	Wear	Pothole
July 2019	Minimum	50%	0.0
	Maximum	100%	0.0
	Average	71.43%	0.0
	Standard Deviation	26.73	0.0
August 2020	Minimum	50%	0.0
	Maximum	100%	0.03%
	Average	71.43%	0.005%
	Standard Deviation	26.73	0.01

Table 9. Statistical values of distortion and connection densities in metal railing of RC bridges inspected in 2019

Date	Value	Distortion	Connection
July 2019	Minimum	0.38%	0.0
	Maximum	15%	0.69%
	Average	5.00 %	0.34%
	Standard Deviation	5.27	0.33

Table 10. Statistical values of cracks, delamination and spalling density in median barrier of RC bridges inspected in 2019 and 2020

Date	Value	Cracks	Delamination	Spalling
July 2019	Minimum	0.0	0.0	0.0
	Maximum	1.89%	0.0	6.82%
	Average	0.32%	0.0	1.97%
	Standard Deviation	0.77	0.0	3.11
August 2020	Minimum	0.0	0.0	0.0
	Maximum	5.03	3.14%	6.82%
	Average	0.84%	0.52%	1.97%
	Standard Deviation	2.05	1.28	3.11

Table 11. Statistical values of wear density in RC curbs and sidewalks of RC bridges inspected in 2019 and 2020

Date	Value	Wear	Spalling	Settlement
July 2019	Minimum	0.0	0.0	0.0
	Maximum	99.33%	5.00%	99.33%
	Average	69.83%	1.60%	28.15%
	Standard Deviation	47.73	1.74	48.07
August 2020	Minimum	0.0	0.0	0.0
	Maximum	99.33%	5.00%	99.33%
	Average	65.19%	1.48%	16.56%
	Standard Deviation	50.52	1.88	40.55